CrossMark

ORIGINAL ARTICLE

Gaseous electron multiplier gain characteristics using low-pressure Ar/CO$_2$

T. Rogers[1] · R. McEntaffer[2] · T. Schultz[2] ·
J. McCoy[2] · D. Miles[2] · J. Tutt[2]

Abstract Gaseous Electron Multiplier detectors, or GEMs, show promise for use on space-based X-ray missions. Operating pressure strongly affects the gain of the detector and must be optimized for best performance. We have measured the gain characteristics of a GEM detector at various pressures below atmosphere using a mixture of Ar:CO$_2$ with the goal of maximizing gain to push GEM capabilities to the lowest energies possible. This paper discusses our tests, results, and their implications for choosing a detector pressure. We found that at any operating pressure the detector voltage can be adjusted to achieve roughly the same maximum gain prior to the onset of electrical discharges. We also find that the gain varies substantially by spatial location across the detector, but this variation is insensitive to changes in pressure allowing it to be calibrated and corrected if necessary. The detector pressure can therefore be optimized in the interest of other performance parameters such as leak rate, window stress, power requirements, or quantum efficiency without concern for negatively affecting the gain. These results can inform the choice of operating pressure and voltage for GEMs used onboard future space missions.

✉ T. Rogers
thomas.rogers@colorado.edu

R. McEntaffer
rlm90@psu.edu

[1] University of Colorado, 1255 38th St. Boulder, CO 80303, USA

[2] Pennsylvania State University, 525 Davey Lab, University Park, PA 16802, USA

1 Introduction

In recent years, Gaseous Electron Multipliers (GEMs) have been considered for their potential use as X-ray detectors for space-based missions ([2, 8–10, 14]). GEMs were originally developed at CERN by [12] and have been studied extensively for their use as particle and X-ray detectors. Achieving desirable detector characteristics is difficult for a space mission, as they must achieve optimal performance while being rugged enough to survive launch (and possibly reentry), vacuum, and the general space environment. Requirements will also change based on the specific goals of a mission.

Gas pressure is one of the most important operational parameters to optimize for a GEMs-based space mission as it directly affects the gas leak rate, stress on thin windows, quantum efficiency, electron diffusion (for polarimeters), and gain. Detector gain must be high enough to ensure that photo-electron pulses are detectable, often a difficult prospect when working with soft X-rays below 1 keV. Unfortunately, increasing the gain also increases the risk of electrical discharges inside the detector. Small discharges can produce false signal inside the detector, typically manifesting as "hot spots" that dominate the signal in localized areas of the detector. Large discharges can cause permanent damage to the detector. Thus, it is important for the gain to be both high enough to detect all photo-electron pulses and low enough to avoid excess noise and detector damage. The two principle variables which control GEM gain are applied voltage (between/across GEM foils) and gas pressure.

We seek to demonstrate the gain characteristics of a GEM detector filled with Ar:CO_2 (75:25 ratio) below atmospheric pressure. Our goal is to generate the highest gain possible, allowing reliable detection of low-energy X-rays ($<$ 1 keV). Our work differs from previous investigations by utilizing a detector with four GEM foils (see Section 2 for further explanation) and producing spatial gain maps at different pressures. Previous investigations of GEM gain have largely been carried out at or above atmospheric pressure ([5, 12, 15]) or have utilized gas mixtures other than Ar:CO_2 ([6, 7, 13]). Bondar et al. [3] investigated the gain characteristics of a 3×3 cm^2 GEM detector with a single internal GEM foil using high- and low-pressure Ar:CO_2. Our 10×10 cm^2 detector amplifies the electron signal with four GEM foils and achieves higher gain values as a result. Additionally, our investigation includes the variation in gain across the face of the detector (gain maps) at several different gas pressures.

In the present work, we systematically study the effect of gas pressure on a detector's gain characteristics. Our tests were carried out below atmosphere, as this pressure range is relatively unexplored and can provide enhanced quantum efficiency (by allowing thinner detector windows) or longer mission lifetimes (via lower leak rate for very thin windows). The results can be used to inform the decision of operational parameters. In Section 2 we discuss our experimental setup and procedures. Section 3 discusses our methods for calculating the gain. Section 4 presents our results, and Section 5 concludes with a discussion of our results and their implications.

2 Experiment setup and procedure

GEM detectors produce gain using a series of foils which consist of a perforated layer of dielectric material that is copper-coated on both sides. Applying a voltage difference between the copper layers induces a large electric field within the pores which serves to amplify an incident charge cloud. In a GEM detector, an X-ray enters the detector through a thin window and ionizes the gas, producing a population of photoelectrons. The photoelectrons drift in an applied electric field towards the GEM foils and are accelerated through the pores causing additional ionizations and thus amplifying the signal.

We use a gas mixture of $Ar:CO_2$ (75:25). As a monatomic gas with no rotational or vibrational states, Ar is efficiently ionized by incident X-rays. When compared to other noble gases, which can all be used in GEM detectors, Ar produces a relatively large number of initial photoelectrons while also being inexpensive. Pure Ar is not an ideal detector gas, because ionized Ar atoms emit radiation when they recombine that can ionize the Cu GEM foils leading to constant discharge. The CO_2 in our detector acts as a quenching agent by collisionally de-exciting recently recombined Ar atoms. This allows higher gains to be reached before electrical breakdown occurs.

Our detector uses a series of four GEM foils, rather than the 1-3 used in previous work ([5, 7, 12, 15]). Our foils are procured from SciEnergy and consist of laser-etched, copper-coated, Liquid Crystal Polymer (LCP). The laser-etching process has been shown to be superior to acid etching by producing cleaner and more consistent pore shapes, thus reducing the risk of electrical breakdown ([15]). LCP is used as the dielectric due to its lower hygroscopicity than polyimide, which is also often used ([5, 12]). The active area of each foil is 100×100 mm^2 with 70 μm diameter holes at 140 μm pitch. The LCP is 100 μm thick with 5 μm layers of Cu on each side.

Our detector assembly is shown schematically in Fig. 1. X-rays enter the detector through a thin window (5000 Å polyimide with 300 Å carbon coating) and ionize gas in the 5 mm-thick drift region in front of the GEM foils. The drift region is followed by the four GEM foils with 1.5 mm gaps between each foil. There is a final 1.5 mm gap between the final foil and the detector anode.

The GEM foils are followed by an anode which collects the charge created inside the pores. The detector anode is a two-layer serpentine cross delay line, shown in Fig. 2. One trace runs back and forth horizontally, the other vertically. A charge cloud from the 4 GEM foils is deposited onto the traces and then runs in all directions (up, down, left, and right) to the terminals at each end. This creates a voltage pulse at each terminal. The position of the incident charge cloud (and the X-ray that produced it) can be determined based on the relative timing of the voltage pulses at the terminals. For instance, a charge cloud incident on the center of the anode will create pulses which reach the terminals simultaneously, whereas a cloud incident on a corner will produce an immediate set of two pulses followed by an additional two that are delayed by the travel time through the traces. The terminals are connected to preamplifiers which ultimately feed a Time-to-Digital Converter (TDC). The TDC converts the analog timing data into a digital spatial position for each photon.
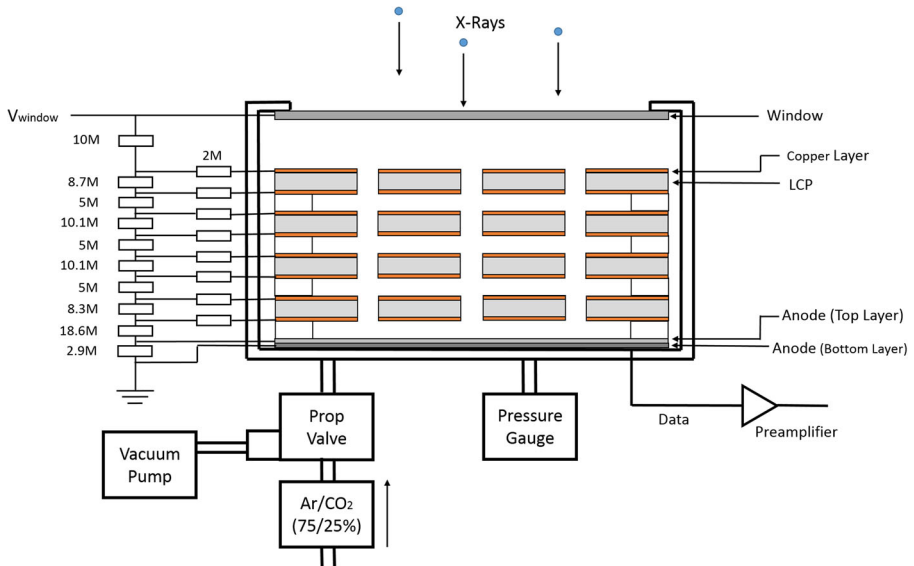
Fig. 1 Our detector setup is shown above in schematic format (not to scale). Light enters the gas-filled chamber through a thin window and ionizes the gas molecules, producing photoelectrons. The photoelectrons are accelerated through the pores of the four GEM foils amplifying the signal. The resulting electron cloud is deposited on the two-layer cross delay-line anode and sent to the electronics. Detector pressure is controlled and maintained with a proportional valve

A resistor chain (see Fig. 1) maintains voltage differences between the window, each copper layer, and the anode. There are 10 MΩ across the initial drift region, 8.7 MΩ across the first foil, 10.1 MΩ across the second and third, 8.3 MΩ across
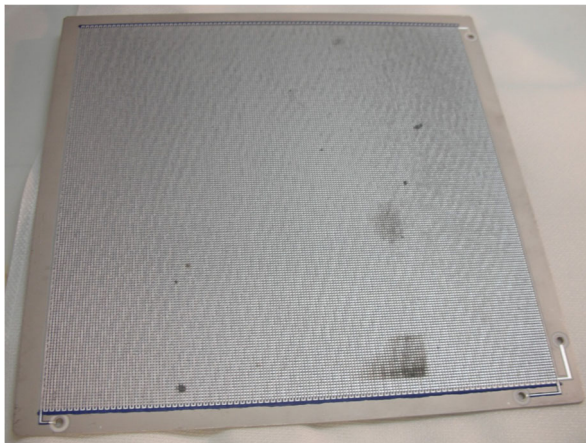

Fig. 2 The detector anode is a two-layer cross delay line. One trace runs back and forth horizontally. The other runs vertically. The circular terminals on the right and bottom edges connect to the preamplifiers. The *black marks* seen on this anode are the result of electrical breakdown inside the detector

the fourth, and 18.6 MΩ across the final drift region to the anode. A resistance of 5 MΩ is held across the drift regions between foils. There are 2.9 MΩ held between the top and bottom layers of the detector anode. As the bottom layer of the anode is partially obscured by the top layer, it tends to absorb fewer electrons. The resistance between anode layers maintains a voltage difference which serves to counter-act this geometry effect by attracting more electrons onto the bottom layer. To minimize the damage from potential electric discharges between copper layers, a 2 MΩ protection resistor is added in series with each GEM electrode.

Depending on the test, signal from the preamplifiers was either fed directly into an oscilloscope for immediate inspection, or sent to the TDC. The oscilloscope was used to monitor the size of amplified charge pulses. The TDC converted the timing of charge pulses into physical location coordinates on the anode to create an image. The TDC also digitized each charge pulse and assigned a value to the total charge level. House-keeping data (temperature, detector pressure, and applied voltage) were also collected.

Impurities in the detector gas can lower gain. Thus, the detector was evacuated and flushed with gas to remove water and impurities prior to testing. Evacuation occurred overnight to ensure that impurities were removed sufficiently. During testing, the detector pressure was maintained using a pressure-sensitive proportional valve. The detector was mounted to a vacuum chamber to maintain outward pressure on the thin detector window, even when operating below atmosphere. A Fe-55 source was installed inside the chamber to provide X-rays.

Temperature has been shown to effect the gain of GEM detectors ([16]). Our testing was carried out at room temperature which was constantly monitored to allow correction of the measured detector gain. Temperature correction proved to be unnecessary, as the laboratory remained at a constant 74 °F (23 °C) for the duration of our tests.

3 Gain theory

The effective gain of a detector is typically defined as

$$G_{eff} = C \times \frac{S_{mean}}{q_e n_e}, \tag{1}$$

where S_{mean} is the average measured pulse height, q_e is the electron charge (1.602×10^{-19} Coulombs), and n_e is the number of initial photoelectrons created by the absorption of an X-ray ([17]). The constant, C, represents the calibration between the amount of input charge and the voltage peak of a charge pulse measured on the oscilloscope (or the charge channel when using the TDC). This constant has units of [C/V], ensuring that the gain is unitless. G_{eff} includes losses within the gas, foils, and anode.

Because our detector anode has two distinct layers which collect unequal amounts of charge (which are subsequently fed into separate amplification channels), we will define our effective gain as

$$G_{eff} = C_1 \times \frac{S_{1mean}}{q_e n_e} + C_2 \times \frac{S_{2mean}}{q_e n_e} \tag{2}$$

where the subscripts refer to the layers of the anode. The mean value of n_e is $\sim$ 215 for a 5.9 keV Fe-55 X-ray and a mixture of 75 % Ar and 25 % CO_2 ([11]). We determined the values of C_1 and C_2 by feeding a 1 V square pulse (10 μs wide, 90 ns rise time, 10 ns fall time) through a 1 pF capacitor to deposit a known amount of charge (1 pC) into the preamplifier channels and measuring the size of the resulting pulse heights in each channel.

4 Gain measurements

To determine the effect of detector pressure on gain, we measured the average gain of the detector at several pressures (7.5, 10, 12.5, and 15 psi) at a range of applied voltages. We created gain maps at these pressures to test whether the gain in certain areas of the detector was affected more strongly than in others. Finally, we measured the gain stability by taking periodic gain measurements for an hour in order to ensure that our detector would be stable over the course of our various tests.
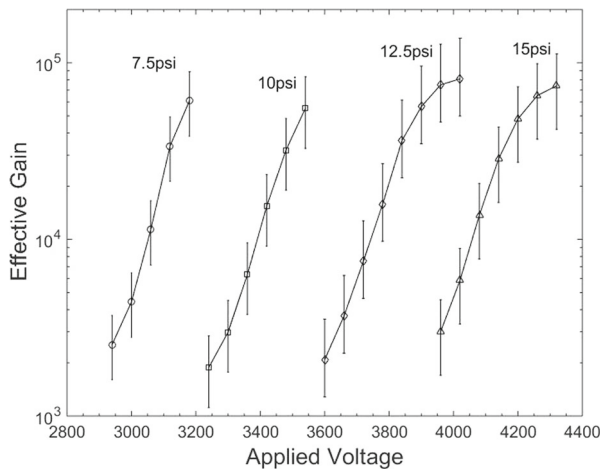

Fig. 3 Gain can be increased by lowering the gas pressure or increasing the voltage applied across the detector's resistor chain. However, the maximum achievable gain is very similar between different pressures. Gain varies substantially by location across the detector. The *bars* enclose 68.2 % of this spatial variation

4.1 Gain curves

The average gain across the detector was measured with an oscilloscope at different pressures. The results are shown in Fig. 3 for various voltages applied to the detector resistor chain. Due to spatial variations in gain (discussed in Section 4.2), the size of pulses measured by the oscilloscope can vary widely (seen as the bars in Fig. 3), so incoming pulses must be time-averaged to produce a useful measurement. Voltage was increased at each pressure until electrical discharge occurred to determine the maximum achievable gain. We attempted gain measurements at 2.5, 5, 7.5, 10, 12.5, and 15 psi. At 2.5 and 5 psi, discharge events occurred while the gain was still too low to be accurately measured.

Slightly higher gains were measured at 12.5 and 15 psi than at 7.5 and 10 psi. However, when large voltages were applied at these pressures (>3900 V at 12.5 psi
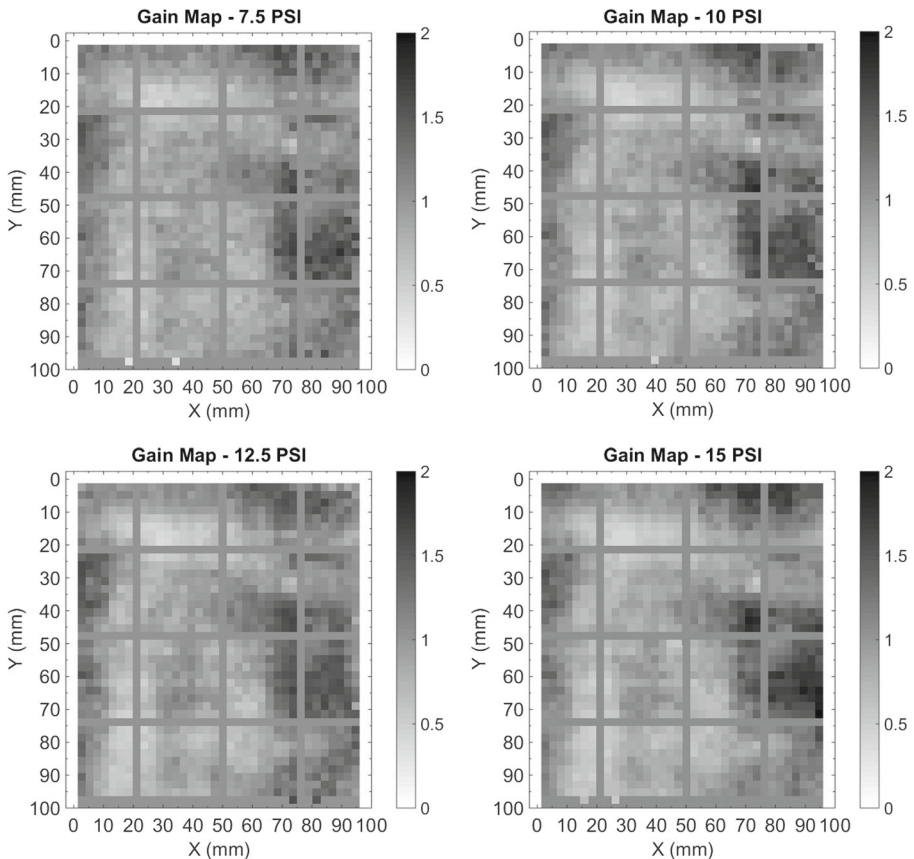

Fig. 4 Gain varies substantially by location on the detector. *Dark areas* on the *left*, *top*, and *right sides* of the detector have ~4-5 times the gain of the lightest areas. The spatial variation in gain remains constant at different pressures, and the total range in gain across the detector undergoes only mild changes. The 4 × 4 grid pattern overlays the area shadowed by the detector's window support structure and has not been included in the gain maps due to its low count rate

and >4200 V at 15 psi), very large voltage spikes began to appear on the oscilloscope. These spikes were off the scale of the oscilloscope's y-axis and were clearly not in-family with the typical pulses arriving due to photon absorption. These pulses signal the appearance of minor discharges between foils. Thus, the highest attainable gains at 12.5 and 15 psi are not useful in practical terms, as they are accompanied by the appearance of very large pulses, greatly increasing the background signal of the detector. The authors chose not to increase the applied voltage further out of fear of damaging the detector. Thus, the maximum achievable gain prior to the degradation of performance is very similar (5-6 $\times$ 10^4) at different pressures.

4.2 Gain maps

Gain maps at various pressures are shown in Fig. 4. These maps were taken at 7.5, 10, 12.5, and 15 psi. To produce an image, charge pulses were fed into the TDC rather than the oscilloscope. The TDC measured the height of each pulse, assigning a value between 0-255. Applied voltages were 3036 V (7.5 psi), 3384 V (10 psi), 3732 V (12.5 psi), and 4020 V (15 psi). These voltages were chosen so that the average pulse height had a value close to 128, preventing large spikes in channels 0 and 255.

The 4 $\times$ 4 grid pattern on each image corresponds to regions behind the window's aluminum support structure, which blocks light and leads to areas of very low count rate. We have masked these areas so that they do not affect the color scaling of the gain maps. The color bars on these maps have been scaled such that the average gain for each map has a value of 1.

Gain varies substantially across the detector face spanning values from roughly 0.3 – 1.8 for each map (also illustrated by the large bars in Fig. 3). This range of values does not change appreciably at different pressures, nor do the positions of high/low gain regions.
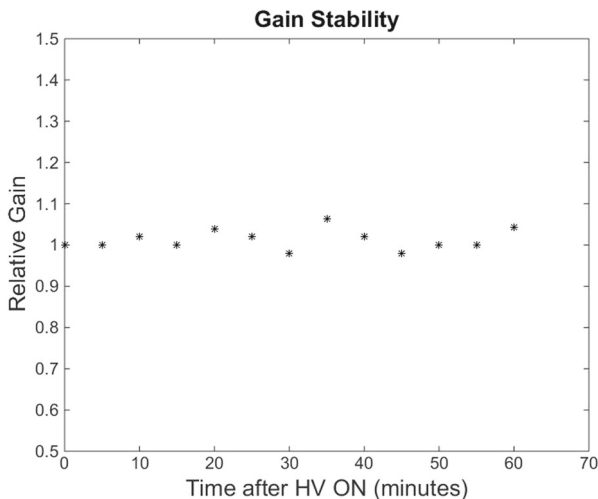

Fig. 5 The gain is very stable over the period of an hour. No ramp-up time is required to achieve full gain, and the gain remains stable to within $\pm$ 5 %

4.3 Gain stability

A plot of gain over the course of an hour is shown in Fig. 5. The measurements were taken at a pressure of 10 psi and a voltage of 3576 V. It has been shown that LCP GEMs are stable over long time periods ([15–17]). We monitored the gain of our detector (as well as temperature, pressure, and voltage) for 1 hour in increments of 5 minutes. The spatially-averaged gain was stable, varying by $< \pm 5$ %, far below the level of the spatial variations seen in the gain maps.

5 Conclusions

We find that the maximum achievable gain is roughly constant with pressure. Higher gas pressures lower the gain (for a given voltage) but also make the detector less prone to arcing. Thus, higher voltages can be applied at higher pressures, and comparable gains can be reached (though this not necessarily true for different gas mixtures; [4] found different behaviors for Ne, Ar, and Xe at high pressures). Detector pressure, therefore, does not affect the maximum achievable gain. This will allow GEM-based space missions to optimize the detector pressure with respect to other mission parameters such as leak rate (and thus mission life-time), window thickness, power requirements, or quantum efficiency.

Gain varies substantially across the face of the detector, but this spatial variation does not change with gas pressure. The presence of strong spatial variation is likely due, in part, to the large size of our detector, allowing more opportunity for variation than a smaller detector would produce (see the results from [17] for comparison to a 9×9 mm^2 region at atmospheric pressure). Possible sources of this variation are the foils themselves (spatial variation in their electron amplification) and the detector anode (spatial variation in its ability to absorb electrons). A natural follow-up test would be to rotate the GEM stack relative to the anode and see whether the features of the gain maps rotate as well. Unfortunately, our detector setup only allows the GEM stack to be mounted in a single orientation, making this test impossible, at present. Bellazzini et al. [1] illuminated a single GEM with a narrow beam of X-rays and used picoammeters to measure the current at each electrode. This method, combined with a motorized stage could also be used to map the gain of the GEMs in the absence of our anode. Regardless of the ultimate source of the spatial variations, their insensitivity to pressure allows the detector pressure to be optimized without fear of changing the gain characteristics. The permanence of the gain maps also allows the variations to be calibrated and corrected during data reduction.

We also find that the gain is very stable in time, showing no substantial changes in gain in the hour after turn-on, in agreement with previous experiments with LCP GEM foils ([15]). Immediate stability after turn-on is an important aspect, as this will allow GEM detectors to be turned off for a period (passing through the South Atlantic Anomaly, for instance) and then turned back on again with no wait-time required between turn-on and data acquisition.

The fact that maximum achievable gain and gain maps do not change with pressure can allow an Ar:CO$_2$-filled detector to be optimized for quantum efficiency, window

thickness, or operational voltage, without concern for the gain that will ultimately be achievable. Space missions utilizing GEM detectors should thus consider these results while designing their detector systems.

References

1. Bellazzini, R., Brez, A., Gariano, G., Latronico, L., Lumb, N., Spandre, G., Massai, M., Raffo, R., Spezziga, M.: What is the real gas gain of a standard gem? Nucl. Instrum. Methods Phys. Res. **419**, 429–437 (1998)
2. Bellazzini, R., Costa, E., Matt, G., Tagliaferri, G.: A polarimeter for ixo. In: X-ray Polarimetry: A New Window in Astrophysics. Cambridge University Press (2010)
3. Bondar, A., Buzulutskov, A., Sauli, F., Shekhtman, L.: High- and low-pressure operation of the gas electron multiplier. Nuc. Inst. Methods Phys. Res. **419**, 418–422 (1998)
4. Bondar, A., Buzulutskov, A., Shekhtman, L.: High pressure operation of the triple-gem detector in pure ne, ar and xe. Nucl. Instrum. Methods Phys. Res. **481**, 200–203 (2002)
5. Bressan, A., Buzulutskov, A., Ropelewski, L., Sauli, F., Shekhtman, L.: High gain operation of gem in pure argon. Nuc. Inst. Methods Phys. Res. **423**, 119–124 (1999)
6. Chechik, R., Breskin, A., Garty, G., Mattout, J., Sauli, F., Shefer, E.: First results on the gem operated at low gas pressures. Nuc. Inst. Methods Phys. Res. **419**, 423–428 (1998)
7. Cortesi, M., Yurkon, J., Stolz, A.: Operation of a thgem-based detector in low-pressure helium. J. Instrum., 10 (2015)
8. Costa, E., Soffitta, P., Bellazzini, R., Brez, A., Lumb, N., Spandre, G.: A efficient photoelectric x-ray polarimeter for the study of black holes and neutron stars. Nature **411**, 662–665 (2001)
9. Jahoda, K.: The gravity and extreme magnetism small explorer. Proc. SPIE, 7732 (2010)
10. Rogers, T., McEntaffer, R., Schultz, T., Zeiger, B., Oakley, P., Cash, W.: The ogress sounding rocket payload. Proc. SPIE, 8859 (2013)
11. Sauli, F.: Principles of operation of multiwire proportional and drift chambers. Lect. Acad. Train. Program CERN, 77–09 (1977)
12. Sauli, F.: Gem: A new concept for electron amplification in gas detectors. Nucl. Instrum. Methods Phys. Res. **386**, 531–534 (1997)
13. Shalem, C., Chechik, R., Breskin, A., Michaeli, K., Ben-Haim, N.: Advances in thick gem-like gaseous electron multipliers part ii: Low-pressure operation. Nuc. Inst. Methods Phys. Res. **558**, 468–474 (2006)
14. Soffitta, P.: Xipe: the x-ray imaging polarimetry explorer. Exper. Astron. **36**, 523–567 (2013)
15. Tamagawa, T., Tsunoda, N., Hayato, A., Hamagaki, H., Inuzuka, M., Miyasaka, H., Sakurai, I., Tokanai, F., Makishima, K.: Development of gas electron multiplier foils with a laser etching technique. Nuc. Inst. Methods Phys. Res. **560**, 418–424 (2006)
16. Tamagawa, T., Hayato, A., Abe, K., Iwamoto, S., Nakamura, S., Harayama, A., Iwahashi, T., Makishima, K., Hamagaki, H., Yamaguchi, Y.: Gain properties of gas electron multipliers (gems) for space applications. Proc. SPIE, 7011 (2008)
17. Tamagawa, T., Hayato, A., Asami, F., Abe, K., Iwamoto, S., Nakamura, S., Harayama, A., Iwahashi, T., Konami, S., Hamagaki, H., Yamaguchi, Y., Tawara, H., Makishima, K.: Development of thick-foil and fine-pitch gems with a laser etching technique. Nuc. Inst. Methods Phys. Rese. **608**, 390–396 (2009)